Further constraints on the diagenetic influences and salinity effect on Globigerinoides ruber (white) Mg/Ca thermometry : implications in the Mediterranean Sea

A. Sabbatini, F. Bassinot, S. Boussetta, A. Negri, H. Rebaubier, F. Dewilde, J. Nouet, N. Caillon, C. Morigi

Geochemistry Geophysics Geosystems G3

Article
Volume 12, Number 10
14 October 2011
Q10005, doi:10.1029/2011GC003675
ISSN: 1525-2027

Published by AGU and the Geochemical Society

Further constraints on the diagenetic influences and salinity effect on *Globigerinoides ruber* (white) Mg/Ca thermometry: Implications in the Mediterranean Sea

Anna Sabbatini
Dipartimento di Scienze della Vita e dell'Ambiente, Università Politecnica delle Marche, Via Brecche Bianche 60, I-60131 Ancona, Italy (a.sabbatini@univpm.it)

Franck Bassinot
Laboratoire des Sciences du Climat et de l'Environnement, CNRS/CEA/UVSQ, Domaine du CNRS, Avenue de la Terrasse, Bat. 12, F-91198 Gif-sur-Yvette CEDEX, France (franck.bassinot@lsce.ipsl.fr)

Soumaya Boussetta
Laboratory GEOGLOB, FSS, University of Sfax, Route de Soukra, BP 802, 3028 Sfax, Tunisia (soumaya.boussetta@lsce.ipsl.fr)

Alessandra Negri
Dipartimento di Scienze della Vita e dell'Ambiente, Università Politecnica delle Marche, Via Brecche Bianche 60, I-60131 Ancona, Italy (a.negri@univpm.it)

Hélène Rebaubier and Fabien Dewilde
Laboratoire des Sciences du Climat et de l'Environnement, CNRS/CEA/UVSQ, Domaine du CNRS, Avenue de la Terrasse, Bat. 12, F-91198 Gif-sur-Yvette CEDEX, France (helene.rebaubier@lsce.ipsl.fr; fabien.dewilde@lsce.ipsl.fr)

Julius Nouet
UMR IDES 8148, Université Paris-Sud 11, F-91405 Orsay, France (julius.nouet@u-psud.fr)

Nicolas Caillon
Laboratoire des Sciences du Climat et de l'Environnement, CNRS/CEA/UVSQ, Domaine du CNRS, Avenue de la Terrasse, Bat. 12, F-91198 Gif-sur-Yvette CEDEX, France (nicolas.caillon@lsce.cnrsgif.fr)

Caterina Morigi
Stratigraphy Department, Geological Survey of Denmark and Greenland, Øster Voldgade 10, DK-1350 Copenhagen, Denmark (cmor@geus.dk)

[1] We analyzed Mg/Ca ratios of the planktonic species *Globigerinoides ruber* (white) picked from 49 box core samples covering the whole Mediterranean Sea and 2 core tops from the Atlantic Ocean. Over the entire data set, we found no significant correlation between Mg/Ca and δ^{18}O-derived calcification temperatures. This lack of correlation is chiefly due to the presence of an early diagenetic, Mg-rich calcite coating, which can constitute up to 20% of the total shell calcite in the central and eastern Mediterranean basin and result in anomalously high Mg/Ca values and a high scattering. In the western Mediterranean Sea, however, *G. ruber* Mg/Ca scattering shows smaller amplitude and Mg-rich calcite remains under the XRD detection limit. SEM observations indicate that only a few samples are affected by trace amounts of *post-mortem* calcite overgrowths (most of this calcite being likely removed during the chemical cleaning for Mg/Ca analyses). Using core top sediments from the western Mediterranean Sea, we performed an empirical

calibration exercise, which confirms that *G. ruber* Mg/Ca is not only related to temperature but it is also significantly affected by sea surface salinity. This salinity effect is not specific to high salinity environments such as the Mediterranean Sea, since it appears to be coherent with recent results obtained on Indo-Pacific and Atlantic surface sediments, which suggest that a +1 (psu) change in SSS results in a +1.7°C Mg/Ca-temperature bias. This sensitivity to salinity is significantly higher than those deduced from culture experiments.

Components: 12,000 words, 7 figures, 3 tables.

Keywords: Mediterranean Sea; early diagenetic calcite coating; foraminiferal Mg/Ca; salinity.

Index Terms: 0424 Biogeosciences: Biosignatures and proxies; 4243 Oceanography: General: Marginal and semi-enclosed seas; 4912 Paleoceanography: Biogeochemical cycles, processes, and modeling (0412, 0414, 0793, 1615, 4805).

Received 27 April 2011; **Revised** 17 August 2011; **Accepted** 26 August 2011; **Published** 14 October 2011.

Sabbatini, A., F. Bassinot, S. Boussetta, A. Negri, H. Rebaubier, F. Dewilde, J. Nouet, N. Caillon, and C. Morigi (2011), Further constraints on the diagenetic influences and salinity effect on *Globigerinoides ruber* (white) Mg/Ca thermometry: Implications in the Mediterranean Sea, *Geochem. Geophys. Geosyst.*, *12*, Q10005, doi:10.1029/2011GC003675.

1. Introduction

[2] Over the past decade, the Mg/Ca ratio of foraminiferal tests has emerged as a promising temperature proxy and Mg/Ca ratios recorded in planktonic foraminiferal tests are frequently used to reconstruct past, surface ocean temperatures [*Mashiotta et al.*, 1999; *Allison and Austin*, 2003; *Eggins et al.*, 2003; *Barker et al.*, 2005; *Waelbroeck et al.*, 2005; *Schmidt et al.*, 2004, 2006; *Levi et al.*, 2007]. Yet, the incorporation of Mg during the calcification of the tests is a complex and imperfectly known mechanism with potential species-dependent effects and non-temperature biases such as those associated to carbonate ion content of seawater [*Russell et al.*, 2004; *Kisakürek et al.*, 2008] or salinity [*Nürnberg et al.*, 1996; *Lea et al.*, 1999; *Kisakürek et al.*, 2008; *Mathien-Blard and Bassinot*, 2009; *Arbuszewski et al.*, 2010].

[3] *Ferguson et al.* [2008] have shown that there is a response of foraminiferal Mg/Ca to salinity in the Mediterranean Sea. The impact of salinity on *G. ruber* Mg/Ca has been also addressed through recent culture experiments [*Kisakürek et al.*, 2008]. Interestingly, the culture experiment indicates a ~5% Mg/Ca increase per psu unit for *G. ruber* [*Kisakürek et al.*, 2008], while Mediterranean core tops reveal a much steeper relationship (16% Mg/Ca increase per psu) associated to a particularly large Mg/Ca data scattering [*Ferguson et al.*, 2008].

[4] This sensitivity to salinity observed in Mediterranean surface sediments is also much higher than that recently evidenced by *Mathien-Blard and Bassinot* [2009], based on core tops from the Indo-Pacific and Atlantic oceans. *Hoogakker et al.* [2009] and *Boussetta et al.* [2011], who worked on core tops from the Red Sea and on superficial samples from the Mediterranean basin, suggested that anomalously high Mg/Ca ratios measured by conventional analysis of planktonic foraminifers from the Mediterranean Sea, could be chiefly related to early diagenetic, high Mg-calcite overgrowths formed from $CaCO_3$ supersaturated interstitial seawater. High-Mg calcite overgrowth (10–20% Mg) is also responsible for the anomalously high Mg/Ca of foraminifers picked from Caribbean sediment cores [*Regenberg et al.*, 2007]. Finally, *van Raden et al.* [2011] recently suggested that anomalously high Mg/Ca measured on two planktonic foraminifers (*G. bulloides* and *G. inflata*) in the Western Mediterranean Sea is due to inorganic calcite coating on the foraminiferal tests. This appears to be in good accordance with earlier microstructural and geochemical studies performed on several pelagic sites (including one from the Mediterranean Sea), which have revealed early diagenesis processes characterized by the deposition of Mg-rich calcite, containing several percent of $MgCO_3$ [i.e., *Sexton et al.*, 2006].

[5] *Nürnberg et al.* [1996] and *Ferguson et al.* [2008] suggested that this early diagenetic encrustation does not alter significantly the geochemical signal of foraminiferal shells, because this Mg-rich calcite is particularly labile and is easily removed with the standard cleaning protocol used to prepare foraminifer shells for trace element analyses. The only noticeable exception was a few samples from

the eastern Mediterranean area in which foraminifer shells did show post-deposition incrustation that resisted cleaning [*Ferguson et al.*, 2008]. *Boussetta et al.* [2011], who proposed the first quantification of this diagenetic calcite by combining trace element and X-ray diffractometry analyses, recently confirmed that overgrowths of high-Mg calcite are particularly abundant in the central and eastern Mediterranean basins.

[6] Since conflicting results have emerged about the salinity effect on planktonic foraminifer Mg/Ca and because the Mg/Ca-thermometer calibration in the Mediterranean Sea could be biased by diagenetic Mg-rich calcite, we decided to: 1/confirm the amplitude and geographic distribution of early diagenetic Mg-rich calcite deposition on Mediterranean planktonic shells; 2/identify the Mediterranean areas – if any – in which this diagenetic imprint does not exist or can be neglected, making it possible to obtain non-biased, foraminiferal shell Mg/Ca data; 3/use these carefully selected data to better constrain the thermal and salinity dependency of *G. ruber* Mg/Ca. For this purpose, we analyzed the Mg/Ca ratios and $\delta^{18}O$ of the spinose species *G. ruber* (white; *sensu stricto*) picked from box corers and core tops retrieved across the entire Mediterranean Sea. Scanning Electron Microscope (SEM) observations and X-ray diffraction analyses were also performed in order to better constrain the *post-mortem*, diagenetic alteration of *G. ruber* shells.

2. Materials and Methods

2.1. The *Globigerinoides ruber* Planktonic Foraminifer Species

[7] *Globigerinoides ruber* is a spinose, shallow-dwelling species and a long-time favorite of many paleoceanographic studies, which seek to reconstruct surface, paleo-hydrographic conditions. As shown by *Thunell* [1978] and, especially by *Pujol and Vergnaud-Grazzini* [1995], *G. ruber* is the dominant planktonic species across all the Mediterranean Sea: its abundance diminishes in the zones of deep water formation, while in the eastern basin it reaches high percentages, from 40% up to 60% in the Ionian and Levantine basin, respectively. The species dominates at depth of 50 to 100 m and it is more abundant at the end of the summer when SST is higher than 24°C (in particular in the Ionian basin, Levantine basin and the Strait of Sicily). During winter the species thrives in deeper waters.

2.2. Samples

[8] Isotopic and trace element analysis were performed on *G. ruber* (white) picked from 49 surface sediment samples (both box corer tops and core tops, see Table 1) spanning the Mediterranean salinity and temperature gradient and 2 box corer tops from the Atlantic Ocean, near the Strait of Gibraltar (Figure 1 and Table 1). The stratigraphic controls (late Holocene or Holocene) of samples which were used in the study by *Boussetta et al.* [2011] (Table 1) were based on radiometric dating, foraminiferal counts and/or $\delta^{18}O$ isotopic stratigraphy, as defined in MARGO [*Kucera et al.*, 2005]. In addition to those samples, most of the new sediment samples used for the present study were collected with sampling devices which are able to retrieve undisturbed surface sediments (multi and box corers). The upper Holocene age of these samples was attested based on $\delta^{18}O$ stratigraphy.

[9] *G. ruber* were picked in the same size fraction (250–315 μm) for paired oxygen isotopic and trace elemental measurements to minimize sample heterogeneity and limit ontogenic effects [*Elderfield et al.*, 2002].

2.3. Geochemical Analyses (Stable Oxygen Isotopes and Mg/Ca)

[10] Oxygen isotopic ratios were measured at the Laboratoire des Sciences du Climat et de l'Environnement (LSCE). Measurements were done on 3 to 7 shells. Shells were ultrasonically cleaned in a methanol bath to remove clays and other impurities. They were roasted under vacuum at 380°C during 45 min to eliminate organic matter. Samples were analyzed with a Finnigan Δ+ mass spectrometer. All results are expressed as $\delta^{18}O$ in ‰ versus V-PDB with respect to NBS 19 and NBS 18 standards. The mean external reproducibility estimated on a powder calcite standard is ±0.05‰.

[11] Trace element analyses were performed at LSCE, a member of an interlaboratory comparison study of calibration standards for foraminiferal Mg/Ca thermometry [*Greaves et al.*, 2008]. About 20–30 specimens per sample (2 replicates) were used for each Mg/Ca measurement. The sample preparation for the analysis of foraminiferal Mg/Ca follows the protocol of *Barker et al.* [2003]. It consists of several ultrasonic treatments in water and then ethanol to remove adhesive clays, and then a reaction with alkali buffered 0.3% hydrogen peroxide at 100°C to remove any organic matter. A very slight acid leaching with 0.001 M nitric acid is

Table 1. Locations of Sediment Samples Used for Analysis of *G. ruber* (white)[a]

Area	Stations	Latitude (N)	Longitude (E)	Depth (m)	Age Control MARGO[a]	Instrument
Atlantic Ocean	VK	34°08.019′	09°33.28′ W	4385	4	box corer
Atlantic Ocean	VM	35°20.008′	08°00.97′ W	1847	4	box corer
Western Mediterranean						
Alboran Sea	V4A	36°47.391′	00°29.066′	2688	4	box corer
Balearic basin	V3C	40°35.744′	05°17.483′	2748	4	box corer
Balearic basin	MD90-901	39°56′84	01°33′52	1560	4	core top
Balearic basin	PSM I 31	37°190033	03°34395		4	box corer
Balearic basin	PSM I 32	37°190033	03°34395		4	box corer
Tyrrhenian Sea	8226	39° 03.78′	15° 23.7′	1045	4	core top
Tyrrhenian Sea	8234	38° 24.41′	13° 10.21′	781	4	core top
Tyrrhenian Sea	8248	40° 21.77′	11° 48.30′	2481	4	core top
Tyrrhenian Sea	KET80-22	40°35′	11°42′5	2430	4	core top
Tyrrhenian Sea	DED87-07	39°41,22	13°34,51	2970	4	core top
Tyrrhenian Sea	KET80-03	38°49′2	14°29′5	1900	2	core top
Tyrrhenian Sea	KET80-19	40°33′	13°21′	1920	3	core top
Gulf of Lion	CI09	42° 41.045′	03° 51.123′	91	4	box corer
Gulf of Lion	MD99-2344	42°02,61	04°09′04	2326	1	core top
Gulf of Lion	KIGC06	41° 58.744′	04° 42.375′	2387	4	box corer
Eastern Mediterranean						
Adriatic Sea	A1	41°48′ 95″	17° 49′ 89″	1195	4	box corer
Adriatic Sea	MD90-917	41°17′	17°37′	1010	1	core top
Adriatic Sea	KET82-16	41°31′	17°59′	1166	1	core top
Adriatic Sea	MD90-916	41°30′3	17°58′ 2	1150	1	core top
Ionian basin	KET80-68	38°06′	17°17,5	1578	4	core top
Ionian basin	8209	37° 50.6′	18° 09.8′	2740	4	core top
Ionian basin	8213	38° 29.86′	18° 23.51′	2803	4	core top
Ionian basin	8214	40° 35.4′	18° 52.1′	800	4	core top
Ionian basin	MD90-918	39°35	18°50	695	4	core top
Strait of Sicily	KET80-37	36°57′	11°39′	740	4	core top
Strait of Sicily	MD04-2797	36°57′	11°40	771	4	core top
Strait of Sicily	560	35°51.27′	14°06.20′	992	4	box corer
Strait of Sicily	561	35°47.89′	12°59.49′	485	4	box corer
Levantine basin	562	32°46.45′	19°11.46′	1390	4	box corer
Levantine basin	563	33°43.07′	23°29.95′	1879	4	box corer
Levantine basin	564	33°00.01′	23°37.77′	1475	4	box corer
Levantine basin	565	34°55.26	23°44.59′	1049	4	box corer
Levantine basin	566	34°27.98′	25°39.96′	1339	4	box corer
Levantine basin	569	33°27.18′	32°34.51′	1294	4	box corer
Levantine basin	571	32°38.87′	34°06.18′	1437	4	box corer
Levantine basin	574	34°26.79′	33°51.77′	1173	4	box corer
Levantine basin	575	34°31.63′	31°47.17′	2337	4	box corer
Levantine basin	576	35°34.41′	30°27.66′	1275	4	box corer
Levantine basin	578	35°29.68′	27°34.53′	1367	4	box corer
Levantine basin	MD84-632	32°47′3	34°22′8	1425	4	core top
Levantine basin	MD84-639	33°40′	32°42′	870	2	core top
Levantine basin	MD84-641	33°02′	32°38′	1375	2	core top
Aegean Sea	582	35°39.71′	26°35.00′	1495	4	box corer
Aegean Sea	584	35°51.80′	25°10.39′	1836	4	box corer
Aegean Sea	589	36°45.23′	26°35.26′	583	4	box corer
Aegean Sea	590	37°16.42′	26°11.54′	580	4	box corer
Aegean Sea	595	38°15.72′	25°06.17′	665	4	box corer
Aegean Sea	596	38°57.29′	24°45.20′	883	4	box corer
Aegean Sea	602	40°13.02′	25°14.40′	1496	4	box corer

[a]Size fraction = 250–315 μm. Chronostratigraphic quality levels ranked from 1 to 4 and corresponding to different levels of uncertainty according to criteria established within the MARGO project (Multiproxy Approach for the Reconstruction of the Glacial Ocean): numbers 1 and 2 indicate radiometric controls within the intervals 0–2 ka and 0–4 ka, respectively; number 3 is used for specific stratigraphic control (like percent of *Globorotalia hirsuta* left coiling); and number 4 represents other stratigraphic constraints [*Kucera et al.*, 2005].

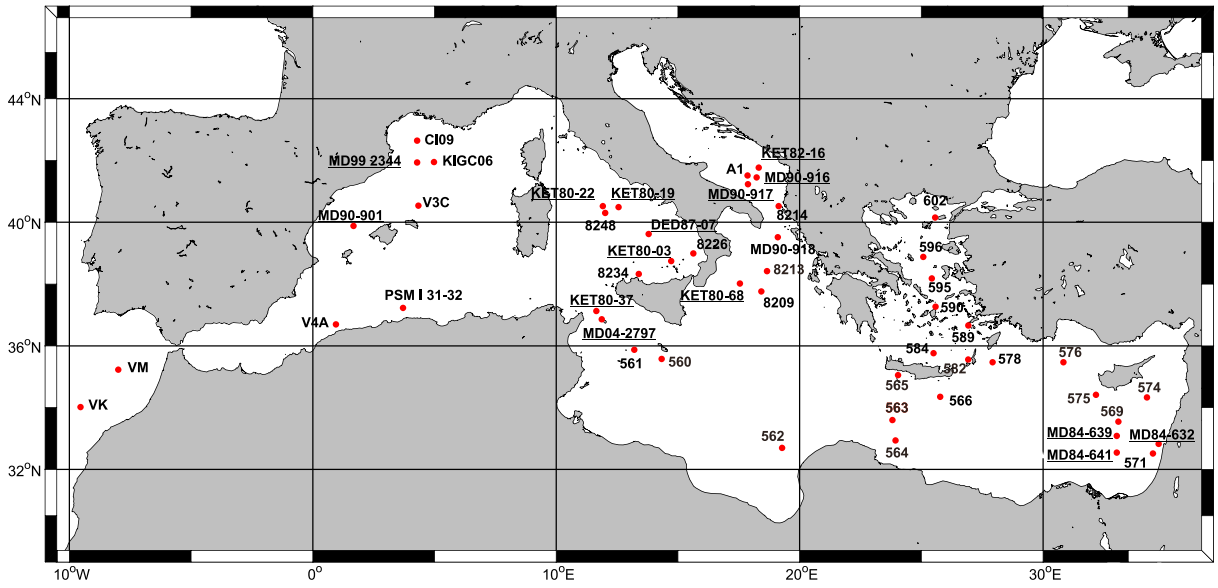

Figure 1. Sample location map. Dark initials mark the locations of the box corer and core tops used in this study and the underlined initials indicate the positions of the analyzed core top samples by *Boussetta et al.* [2011]; in the Table 1 we report all data references.

finally applied to eliminate contaminants adsorbed on foraminiferal tests.

[12] Mg/Ca analyses have been performed on a Varian Vista Pro Inductively Coupled Plasma Atomic Emission Spectrometer (ICP-AES) following the intensity ratio method of *de Villiers et al.* [2002]. The mean external reproducibility obtained on replicate analyses of a standard solution of Mg/Ca = 5.23 mmol/mol is ±0.02 mmol/mol (1 s); that is a relative standard deviation (RSD) of 0.4%. For marine samples, clay minerals are the major source for contamination in Mg/Ca analyses of foraminiferal calcite as shown by *Barker et al.* [2003]. In accordance to these authors, we carefully considered the Fe/Ca and Al/Ca ratios as potential indicator of such a contamination. Samples showing Fe/Ca values higher than 0.10 mmol/mol and Al/Ca values higher than 0.04 mmol/mol were rejected. Samples with Mn/Ca ratios higher than 0.10 mmol/mol were also disregarded in order to eliminate biases associated to oxide coatings.

2.4. X-Ray Diffractometry Analyses

[13] Several samples showed clearly anomalous Mg/Ca values reaching up to 35.5 mmol/mol. Because they are not associated with significant values of Fe, Al and Mn, these anomalous Mg/Ca ratios could not be explained by a terrigeneous contamination (in Figure 1, samples: 560, 563, 564, 569). Specimens of *G. ruber* were extracted from these samples and observed under a scanning electron microscope, and analyzed through X-ray diffractometry (XRD) after having been submitted to a simplified cleaning procedure (ultra-sonification in distilled water) without acid leaching. The powder preparation for XRD analyses follows the protocol of *Nouet and Bassinot* [2007]. Because foraminifera tests weight only a few micrograms, this protocol was developed using a "zero-background," silicon mono-crystalline sample holder that makes it possible to work with minute amounts of powder (around 250 μg). Analyses were performed at IDES (University of Paris Sud, Orsay) on an Xpert Pro from *Panalytical*, equipped with a Cu X-ray tube and a Ni filter that eliminates the Cu K X-ray.

2.5. IGOR® Deconvolution Approach

[14] In order to isolate overlapping peaks that belong to different minerals, profiles obtained from the X-ray diffractometry analyses were deconvolved using the IGOR® package, a more powerful software that the one used by *Boussetta et al.* [2011], and which allows a better control on the peak deconvolution process.

[15] In order to test the IGOR® deconvolution package and estimate uncertainties and limits of our procedure, we generated synthetic, bi-phased calcite diagrams ("pure calcite" + Mg-rich calcite) with known amounts of Mg-rich calcite coating (varying from 0.5 to ~15%), and we used IGOR®

to deconvolve these known, synthetic diagrams using Voigt fitting functions.

[16] Our results indicate that, for the synthetic diagram constructed with 0.5% Mg-rich calcite, this calcite coating goes undetected. Thus, the absence of a detectable Mg-rich peak in our XRD diagrams from Mediterranean samples suggests that the coating is either absent, or below a detectable limit, which is around 0.5%. Our tests also indicate that a 1% coating of Mg-rich calcite can be detected in XRD diagrams and deconvolved with IGOR®, providing that the noise/signal is not too important. However, it is crucial to note that, when the Mg-rich contribution is low, deconvolution of XRD diagrams tends to strongly over-estimate the amount of Mg-rich calcite present. For instance, applied on a synthetic diagram that contains 1% Mg-rich calcite coating, the deconvolution indicates a ~5% content. This overestimation is due to the fact that the deconvolution tends to overestimate the width of very small diffraction peaks (Full Width at Mid-Height, FWMH), resulting in erroneous peak area calculations. With increasing amounts of Mg-rich calcite, the difference between "deconvolved" and "true" contents of Mg-rich decreases, as in shown by the ratio between these two values that tends toward unity (1), as the amount of Mg-rich calcite increases (Figure 2). When the coating corresponds to more than 8–9%, true and deconvolved values are almost identical.

[17] Thus, the lack of detectable Mg-rich calcite peak in the XRD profiles does not prove that diagenesis is not present, it only indicates that the Mg-rich calcite coating corresponds to less than ~0.5% of the foraminifer calcite. In order to get additional constrains on the amount of diagenetic coating on *G. ruber* shells, we conducted detailed Scanning Electron Microscope (SEM) investigations on 9 box corer top samples to look for any evidence of calcitic overgrowths in the western Mediterranean material. *G. ruber* specimens for these analyses were all picked from the superficial sediment (0–0.5 cm depth) and they underwent the normal cleaning process to remove contaminants like clays and coccoliths.

2.6. Calculation of Calcification Salinity and Temperature

[18] In order to discuss the Mg/Ca data and their relationship to SST, *G. ruber* $\delta^{18}O$ and surface seawater $\delta^{18}O$ ($\delta^{18}O_{sw}$) have been combined to estimate the isotopic calcification temperatures. We obtained salinities by averaging *MEDAR Group* [2002] climatological data (http://www.ifremer.fr/medar/) over the appropriate season and depth range corresponding to the peak development of *G. ruber* as observed by *Thunell* [1978] and *Pujol and Vergnaud-Grazzini* [1995]. In addition, we also extracted mean annual salinities for the upper 0–50 m depth range.

[19] For the conversion of salinities to surface water $\delta^{18}O_{sw}$, we used the empirical regression equation developed by *Duplessy et al.* [1991] for our two Atlantic sites (VK and VM):

$$\delta^{18}O_{sw} = (0.558 * \text{salinity}) - 19.264 \quad (1)$$

For the Mediterranean sites, we used the empirical equations developed by *Kallel et al.* [1997]. The modern, seawater isotopic database used by these authors clearly suggests that two regression equations should be used, one for surface salinities <38 (Practical Salinity Unit, psu), and the other for surface salinities >38 (psu).

$$\delta^{18}O_{sw} = (0.41 * \text{salinity}) - 14.18\ S < 38 \quad (2a)$$

$$\delta^{18}O_{sw} = (0.199 * \text{salinity}) - 6.12\ S > 38 \quad (2b)$$

Finally, in accordance with several Mg/Ca-T calibration exercises [i.e., *Anand et al.*, 2003; *Mathien-Blard and Bassinot*, 2009], we used the re-arranged equations from *O'Neil et al.* [1969] and *Shackleton* [1974] to calculate the isotopic temperatures of calcification:

$$T_{iso} = 16.9 - 4.38\left(\delta^{18}O_f - \left(\delta^{18}O_w - 0.27\right)\right) + 0.1\left(\delta^{18}O_f - \left(\delta^{18}O_w - 0.27\right)\right)^2 \quad (3)$$

with $\delta^{18}O_w$ the seawater isotopic composition (see above), and $\delta^{18}O_f$ the isotopic composition of *G. ruber*.

[20] We checked what differences would result from using mean annual $\delta^{18}O_{sw}$ values instead of seasonally weighted $\delta^{18}O_{sw}$ values in order to assess if taking into account *G. ruber* seasonal productivity would significantly alter the correlation of Mg/Ca values to hydrographic parameters. The maximum differences between the absolute annual, 0–50 m mean SSS and those estimated based on the living depth and seasonal distributions [*Thunell*, 1978; *Pujol and Vergnaud-Grazzini*, 1995], are <0.3 (psu). These differences range from −0.26 to +0.18 (psu), with an average absolute value of 0.07 (psu). Based on *Kallel et al.*'s

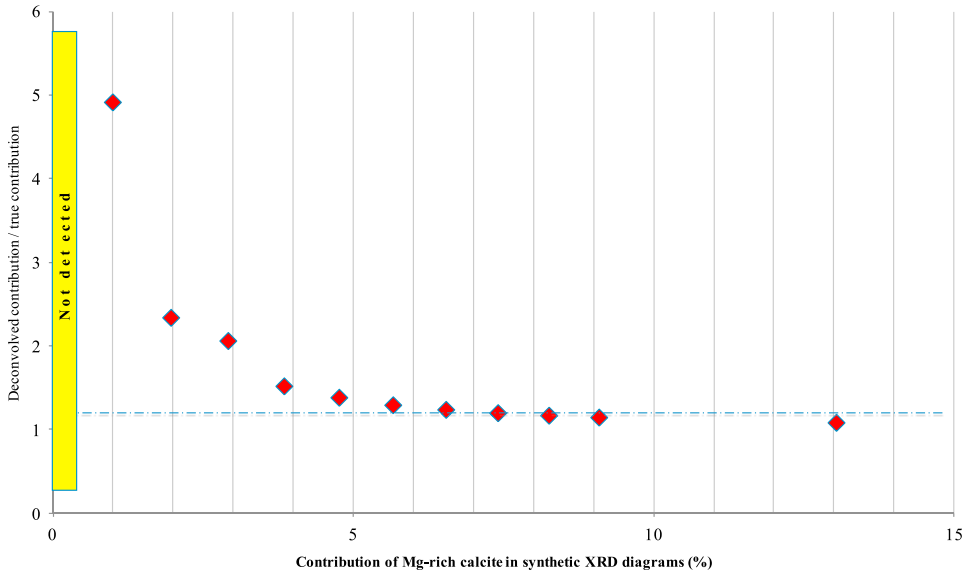

Figure 2. For each synthetic XRD diagram built with two calcite types (pure calcite and Mg-rich calcite), we calculated the ratio between the deconvolved Mg-rich calcite contribution and the true amount of Mg-rich calcite. We plotted this ratio versus the corresponding true Mg-rich calcite contribution for synthetic diagrams containing 0.5 to 15% of Mg-rich calcite. As can be seen in this figure, for samples containing low amount of Mg-rich calcite, deconvolution tends to largely overestimate its contribution.

$\delta^{18}O_{sw}$-SSS empirical relationships [*Kallel et al.*, 1997], those salinity differences translate into differences between annual mean $\delta^{18}O_{sw}$ and productivity-weighted $\delta^{18}O_{sw}$ that are <0.12 (psu) (average = 0.02 (psu)). Using our box corer and core tops, *G. ruber* $\delta^{18}O_f$ data, those seawater isotopic composition differences lead to maximal differences in T_{iso} that are <0.3°C, and average 0.1°C over our database. Because this difference is small, in the present paper, we decided to use T_{iso} obtained from mean annual $\delta^{18}O_{sw}$ (SSS) over the first 50 m depth.

[21] Hydrographic parameters at the location of core top samples, and geochemical data obtained on *G. ruber* are presented in Tables 1 and 2.

3. Results

[22] Most *G. ruber* Mg/Ca ratios fall within the large range 2.6–10.3 mmol/mol, a few even reaching strongly anomalous values as high as 35.5 mmol/mol (see Table 2 and Figures 3 and 4). Given the reconstructed T_{iso} range obtained from *G. ruber* $\delta^{18}O_f$ data at our core top locations (17 to 26°C), our Mg/Ca ratios appear to be high compared to open ocean data published in the literature [*Mashiotta et al.*, 1999; *Anand et al.*, 2003]; yet, they cover the same range of variability than the Mediterranean data from *Ferguson et al.* [2008]. The clearly anomalous Mg/Ca values are obtained principally for core tops located in the central and the eastern basins (Figures 1 and 4). There, Mg/Ca data not only show the highest values (up to 35 mmol/mol), but display also the largest variability (ranging from 3.4 to 35.5 mmol/mol). There is an apparent West-East trend of increasing Mg/Ca ratios (Figure 4).

[23] With no surprise, the presence of numerous, anomalously high Mg/Ca values and the important scattering of the data result in the absence of statistically meaningful relationship between *G. ruber* Mg/Ca and isotopic calcification temperatures (R^2 ~0.003) (Figure 3).

[24] *Boussetta et al.* [2011] using XRD and SEM data, showed and quantified the presence of Mg-riche calcite coating foraminiferal shell from the Mediterranean core top samples. We extended their work by performing XRD analyses on 5 additional box corer tops from the Western Mediterranean Sea (underlined values in Figure 4). The %Mg content of the Mg-rich phase in our samples can be estimated from the angular shift of the main calcite diffraction peak (104) as evaluated in the study by *Boussetta et al.* [2011]. Results indicate that it contains about 10–12% of $MgCO_3$, which is coherent with a calcite phase deposited in equilibrium with seawater Mg and Ca concentrations [*Mucci*, 1987]. Precipitation of carbonate out of

Table 2. Hydrographic Parameters at the Location of Sediment Samples (Box Corer Top and Core Top) and Geochemical Data Obtained on *G. ruber* (white)[a]

Stations	$\delta^{18}O_f$ (‰)	$\delta^{18}O_{sw\ year}$ (‰)	$\delta^{18}O_{w\ season\ and\ living\ depth}$ (‰)	T_{year} (°C)	$T_{season\ and\ living\ depth}$ (°C)	S_{year} (psu)	$S_{season\ and\ living\ depth}$ (psu)	$T_{iso\ year}$ (°C)	$T_{iso\ season\ and\ living\ depth}$ (°C)	Mg/Ca (mol/mol)	$T_{Mg/Ca}$ (°C)	ΔT (°C)
Western Mediterranean Basin												
VK	−0.13	1.11	1.08	19	19	36	36	21	21	2.62	20	−1.67
VM	−0.17	1.05	1.02	18	18	36	36	21	21	2.79	20	−0.84
V4A	0.72	1.10	1.13	18	17	37	37	17	18	3.03	21	3.86
V3C	0.21	1.30	1.36	17	18	38	38	21	21	3.92	24	−0.28
MD90-901	0.54	1.24	1.31	17	17	38	38	19	19	3.84	24	5.05
PSM I 31	−0.43	1.01	0.99	18	20	37	37	22	22	3.03	21	−0.94
PSM I 32	0.28	1.01	0.99	18	20	37	37	19	19	2.66	20	0.83
8226	0.42	1.41	1.33	18	19	38	38	20	20	3.54	23	2.86
8234	0.62	1.40	1.33	18	19	38	38	19	19	3.29	22	2.99
8248	0.19	1.34	1.46	17	19	38	38	21	21	4.26	25	4.19
KET80-22	0.49	1.34	1.33	17	19	38	38	19	19	4.35	25	5.76
DED87-07	0.63	1.33	1.33	18	19	38	38	19	19	3.95	24	5.37
KET80-03	0.66	1.35	1.33	18	19	38	38	19	19	4.02	24	5.60
KET80-19	0.84	1.33	1.33	18	19	38	38	18	18	4.48	26	7.66
CI09	0.60	1.44	1.35	15	17	38	38	19	19	3.13	22	2.13
MD99-2344	0.38	1.40	1.38	15	18	38	38	20	20	3.82	24	3.57
KIGC06	0.88	1.39	1.40	15	18	38	38	18	18	3.85	24	5.93
Eastern Mediterranean Basin												
A1	0.74	1.54	1.56	17	16	38	39	19	19	3.62	23	3.97
8209	0.35	1.52	1.52	18	19	38	38	21	21	4.49	26	4.64
8213	0.21	1.53	1.53	18	19	38	38	22	22	4.53	26	4.06
8214	0.84	1.53	1.51	16	19	38	38	19	19	3.81	24	4.98
MD90-918	0.77	1.52	1.55	18	16	38	39	19	19	4.74	26	7.15
MD90-917	0.64	1.52	1.54	17	18	38	39	20	20	3.40	23	2.92
KET82-16	0.71	1.53	1.53	17	18	38	38	19	19	4.31	25	5.80
MD90-916	0.87	1.53	1.53	17	18	38	38	19	19	3.89	24	5.37
KET80-68	0.48	1.50	1.50	18	20	38	38	20	20	4.87	26	6.24
KET80-37	0.73	1.17	1.17	18	20	37	37	18	18	4.80	26	8.67
MD04-2797	0.48	1.19	1.17	18	20	37	37	19	19	4.87	26	7.62
560	0.93	1.30	1.27	19	22	38	38	17	17	*35.49*	49	31.21
561	−0.18	1.19	1.20	19	21	37	38	22	22	6.26	29	7.44
562	−0.16	1.53	1.56	20	23	38	39	23	23	*12.05*	37	13.26
563	0.96	1.60	1.60	19	21	39	39	18	19	*17.03*	40	21.90
564	0.69	1.58	1.60	20	22	39	39	20	20	*17.75*	41	21.18
565	0.69	1.62	1.62	19	21	39	39	20	20	*10.33*	35	15.02
566	0.67	1.65	1.66	20	23	39	39	20	20	7.89	32	11.79
569	0.54	1.65	1.63	21	22	39	39	21	21	*19.57*	42	21.30
571	−0.15	1.59	1.64	21	24	39	39	24	24	4.88	27	2.95
574	0.12	1.67	1.67	21	22	39	39	23	23	7.43	31	8.49
575	0.52	1.68	1.65	20	21	39	39	21	21	*9.64*	34	13.20

Table 2. (continued)

Stations	$\delta^{18}O_f$ (‰)	$\delta^{18}O_{sw\ year}$ (‰)	$\delta^{18}O_{w}$ season and living depth (‰)	T_{year} (°C)	T_{season} and living depth (°C)	S_{year} (psu)	S_{season} and living depth (psu)	$T_{iso\ year}$ (°C)	T_{iso} season and living depth (°C)	Mg/Ca (mol/mol)	$T_{Mg/Ca}$ (°C)	ΔT (°C)
576	0.26	1.65	1.63	20	20	39	39	22	22	7.93	32	9.96
578	−0.04	1.66	1.66	19	21	39	39	23	23	7.22	31	7.47
582	0.56	1.65	1.64	19	21	39	39	21	21	*13.28*	38	17.09
584	0.15	1.65	1.64	19	21	39	39	22	22	6.70	30	7.56
589	0.22	1.65	1.64	19	20	39	39	22	22	5.14	27	4.96
590	0.45	1.61	1.60	18	20	39	39	21	21	5.15	27	6.23
595	1.18	1.57	1.56	18	20	39	39	17	17	5.52	28	10.49
596	0.81	1.52	1.52	17	19	38	38	19	19	3.83	24	4.96
602	−0.66	1.52	1.56	17	19	38	39	26	26	3.82	24	−1.86
MD84-632	0.66	1.59	1.59	20	23	39	39	20	20	5.63	28	8.26
MD84-639	0.76	1.62	1.62	21	22	39	39	20	19	*12.35*	37	17.31
MD84-641	0.25	1.61	1.61	21	23	39	39	22	22	9.96	34	12.67

[a]Size fraction = 250–315 μm. T and S are extracted from *MEDAR Group* [2002] climatological data (http://www.ifremer.fr/medar/) over the appropriate season and depth range corresponding to the peak development of *G. ruber* as observed by *Thunell* [1978] and *Pujol and Vergnaud-Grazzini* [1995]. In addition, we also extracted mean annual T and S for the upper 0–50 m depth range. To obtain $\delta^{18}O_{sw}$ we used the empirical regression equation developed by *Duplessy et al.* [1991] for our two Atlantic sites and for the Mediterranean sites, we used the empirical equations developed by *Kallel et al.* [1997]. Values of $\delta^{18}O_f$ were measured on *G. ruber*, and the isotopic temperature (T_{iso}) was calculated using an equation from *Shackleton* [1974]. Values of Mg/Ca were measured on *G. ruber*, and the corresponding temperatures ($T_{Mg/Ca}$) were calculated based on calibration from *Anand et al.* [2003] for *G. ruber* in the size fraction 250–315 μm. ΔT is the difference between TMg/Ca and Tiso (see section 2.6 for details). In italics are presented samples where Mg/Ca values are anomalous.

seawater is known to result in the formation of a Mg-enriched phase [e.g., *Wollast et al.*, 1980; *Morse and Mackenzie*, 1990; *Tribble et al.*, 1995; *Tribble and Mackenzie*, 1998; *Gehlen et al.*, 2004].

[25] The relative amount of this Mg-rich calcite (Mg-rich calcite/(Mg-rich + Mg-poor calcite)) has been estimated based on the areas of the two calcite phases in the XRD profiles deconvoluted using the IGOR® software (see above the paragraph 2.5. in the Materials and Methods), a more powerful software that the one used by *Boussetta et al.* [2011], which allows a better control on the peak deconvolution process.

[26] Thus, we re-analyzed the *G. ruber* data from *Boussetta et al.* [2011], and show them here together with the new data gathered for this paper (Table 3). This relative amount (in %) of Mg-rich calcite, obtained for 19 samples in total, has been plotted on a Mediterranean Sea map (Figure 4). The values plotted here are those given directly by the IGOR® software. We did not try to correct for deconvolution overestimation in the low end-member part of the spectrum (Figure 2). As indicated by our initial calibration (see above), the lowest values obtained through deconvolution by IGOR® software (i.e., 3.8; 4.5%) should actually correspond to Mg-rich coatings around ~1%; and the lack of detectable Mg-rich calcite (n.d.) signifies that it should be lower than ~0.5%.

[27] As can be seen from the Figure 4, there are important differences across the Mediterranean Sea.

[28] In the Central and Eastern Mediterranean, high amounts of Mg-rich calcite are measured (>3%), reaching up to ~20% in most locations of the Levantine basin, with extreme values as high as 25.8% (Table 3). Noticeably, it is also in these central and eastern sites that anomalously high (and highly scattered) Mg/Ca ratios were obtained with ICP-AES (i.e., sites 560, 563, 564 and 569 as well as eastern most sites MD84–639, MD84–641 and MD84–632; Figure 4 and Tables 2 and 3). Thus, high and scattered Mg/Ca data together with XRD analyses clearly suggest that Mg/Ca thermometer is strongly biased by early diagenetic deposition of Mg-rich calcite coatings in the central and eastern basins of the Mediterranean Sea. It should be noted, however, that even the highest Mg/Ca ratios measured by ICP-AES (i.e., 35.5 mmol/mol) are much lower than values that could be expected from the contamination of foraminiferal calcite by significant amounts (several weight percent) of a Mg-rich calcite containing 10–12% $MgCO_3$. It is likely, therefore, that during the sample preparation

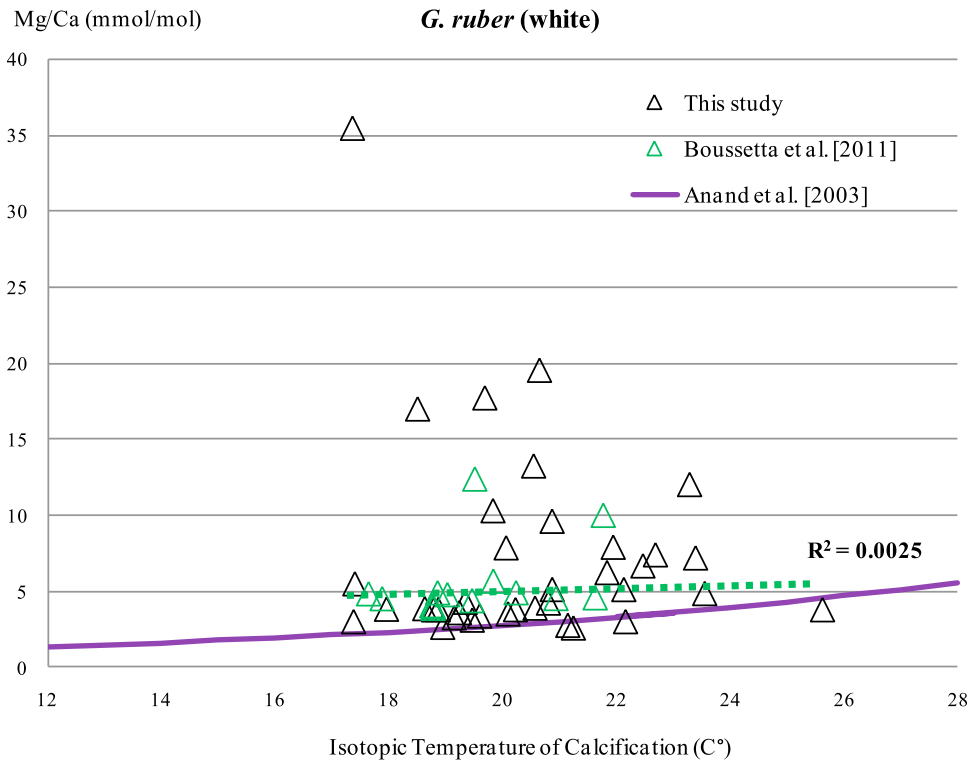

Figure 3. *G. ruber* (white) Mg/Ca ratios plotted against $\delta^{18}O_w$-derived isotopic temperatures calculated using the equations of *Shackleton* [1974] for all Mediterranean samples. The dark triangles represent our Mg/Ca values and the green triangles are Mg/Ca data based on samples from a longitudinal transect in the Mediterranean Sea analyzed by *Boussetta et al.* [2011]. Purple curve is existing calcification temperature calibration for *G. ruber* from the sediment trap series located in the Sargasso Sea; *Anand et al.* [2003] Mg/Ca = $0.449^{e\ 0.09T}$.

for ICP-AES analyses, most of the Mg-rich calcite coating is removed during the acid-leaching step, as was suggested by *Ferguson et al.* [2008]. This hypothesis is supported by the fact that Mg-rich calcite is highly soluble. Several studies have shown that the solubility of Mg-rich coatings formed on calcite seeds during laboratory experiments [*Wollast et al.*, 1980] or in the field [*Morse et al.*, 2003] even exceeds that of aragonite. Yet, opposite to what was concluded by *Ferguson et al.* [2008], our data clearly suggest that Mg-rich coating on *G. ruber* picked from the central and eastern sites cannot be completely removed during the cleaning process, thus explaining the high and scattered Mg/Ca values obtained on those sites. A similar conclusion was reached by *Hoogakker et al.* [2009] who studied downcore sediment samples from the Red Sea and who attributed the high Mg/Ca ratios to coatings and overgrowths resilient to the conventional cleaning procedures. Persistence of overgrowths to routine cleaning procedures has also been observed for Pliocene Caribbean samples [*Regenberg et al.*, 2007; *Groeneveld et al.*, 2008].

[29] In most of the western basins, this Mg-rich calcite is not detected (n.d.) by XRD analysis. Yet, because of the relative high level of noise/signal ratio for several samples, there was a possibility that we could have missed small Mg-rich calcite contributions. Because such a Mg-rich calcite is extremely labile, we decided to check whether we could observe some difference between the original XRD diagrams and those obtained after *G. ruber* shells had been leached with acid. This leaching was performed with the same acid as the one used in the cleaning protocol for Mg/Ca (HNO_3 - 0.001 M), but the duration of the leaching was increased to more than 1 min (instead of ~30 s for the Mg/Ca cleaning procotol) in order to leave more time for the acid digestion to remove Mg-rich coating, if any. We compared XRD diagrams obtained on bulk and leached shells picked from five samples, for which enough material was available. But the results were not conclusive. None of the analyzed samples showed a noticeable difference between its initial and leached XRD profiles. Thus, whether there is or not some Mg-rich coating in the western sites of Mediterranean Sea, it is clearly beyond the detection

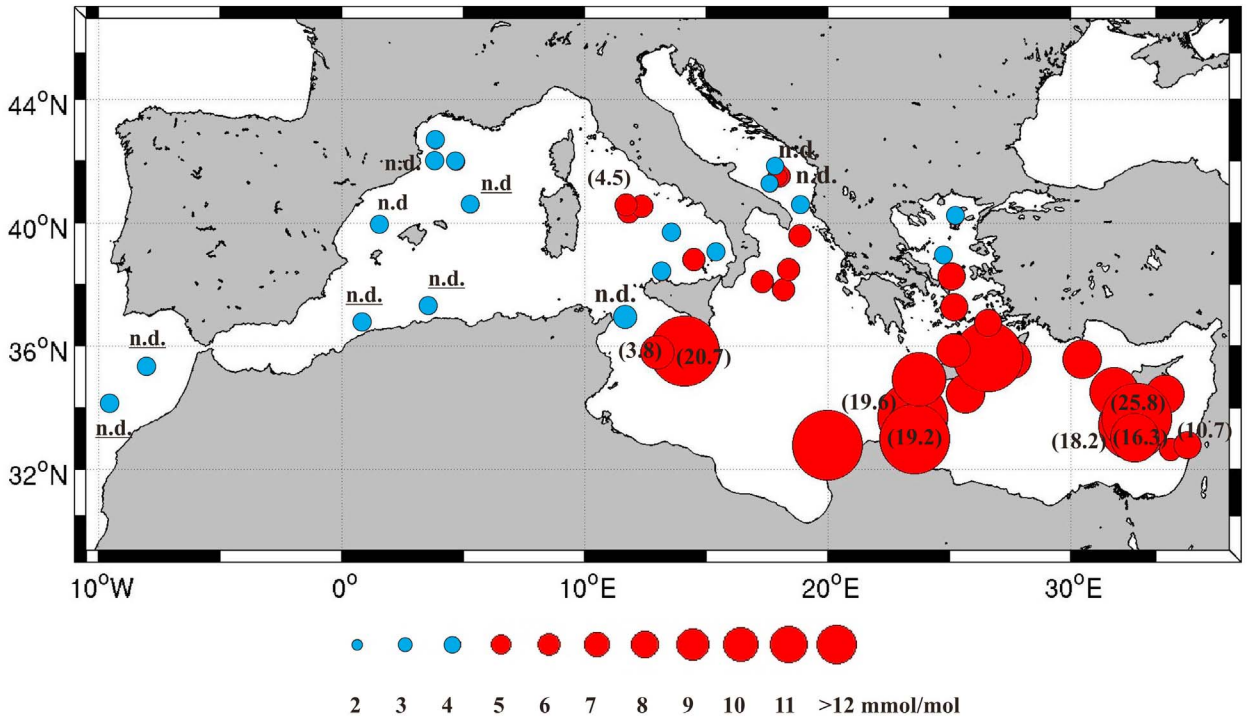

Figure 4. Map showing the geographic distribution of 1) the Mg/Ca ratios measured on *G. ruber* (white) picked from surface sediments as blue (2–4 mmol/mol) and red (>4 mmol/mol) circles; and 2) the relative amount (%) of diagenetic, Mg-rich calcite estimated from XRD analyses (numbers in brackets). Bold numbers correspond to XRD data obtained by *Boussetta et al.* [2011], whereas underlined values are new data from this study. The deconvolution of the main (104) peaks corresponding to the foraminiferal calcite and the Mg-rich calcite, respectively, was performed with the IGOR® software (thus, we re-analyzed data from *Boussetta et al.* [2011]). Mg-rich calcite was not detected (n.d.) in XRD diagrams in most samples from the western Mediterranean Sea. The clearly anomalous Mg/Ca values (large red circles) are obtained principally for samples located in the Levantine basin and its margins, which also show the highest Mg/Ca scattering. It is in this area that we also estimated the highest proportion of Mg-rich calcite from several *G. ruber* (white) samples.

limit of the XRD analyses (~0.5% as shown by our calibration tests).

[30] In order to look for the presence of very low amounts of Mg-rich coating that could have gone undetected through XRD, we performed SEM observations (Figure 5) of the microstructural details of *G. ruber* shells picked from several western Mediterranean samples. Samples from across the Gibraltar strait, in the Atlantic, and from the Alboran sea do not show any sign of diagenetic recrystallization at all (Figure 5, images 1 and 2). Trace amounts of recrystallization were observed on some shells from the Gulf of Lyon and the Tyrrhenian Sea, although pristine specimens could be found as well in nearby samples (Figure 5, images 3–6), indicating that diagenesis remains limited and patchy in these areas (XRD did reveal the occurrence of Mg-rich calcite in a few samples from the Tyrrhenian Sea), But diagenetic alteration is clearly less pronounced here than in central and eastern Mediterranean Sea samples (Figure 5, images 7 and 8). Interestingly, in their core top samples from the Mediterranean basin, *van Raden et al.* [2011] did not observed secondary overgrowths on tests from *Globorotalia inflata*, but only on *Globigerina bulloides*. They observed these overgrowths, for instance, at one site from the Strait of Sicily, located nearby our site 560 for which our SEM analyses show evidence of diagenetical overgrowths on *G. ruber*. Other authors have reported the occurrence of similar overgrowths on *G. ruber*, *G. sacculifer*, *Globorotalia menardii* and *Neogloboquadrina dutertrei* picked in sediments from the Caribbean Sea, the Red Sea, and the eastern Mediterranean [*Regenberg et al.*, 2007; *Ferguson et al.*, 2008; *Groeneveld et al.*, 2008; *Hoogakker et al.*, 2009].

[31] Because of the very limited impact of diagenetic imprints in the samples from the western Mediterranean Sea, we decided to test whether,

Table 3. Results of the Deconvolution of Calcite (104) XRD Peaks for *G. ruber* (white) With the IGOR® Software[a]

Stations	Mg/Ca (mmol/mol)	Percentage of High Mg-Calcite[b]
	Western Mediterranean Basin	
VK[c]	*2.62*	*n.d.*[d]
VM	*2.79*	*n.d.*
V4A[c]	*3.03*	*n.d.*
V3C[c]	*3.92*	*n.d.*
MD90-901	3.84	n.d.
PSM I 31	*3.03*	*n.d.*
KET80-22[c]	4.35	4.5
MD99-2344[c]	3.82	n.d.
	Eastern Mediterranean Basin	
KET82-16	4.31	n.d.
MD90-916	3.89	n.d.
KET80-37	4.80	n.d.
MD04-2797	4.87	3.8
560	35.49	20.7
563	17.03	19.6
564	17.75	19.2
569	19.57	25.8
MD84-632	5.63	10.7
MD84-639	12.35	18.2
MD84-641	9.96	16.3

[a]Size fraction = 250–315 μm. This deconvolution makes it possible to quantify the relative amount of Mg-rich calcite (diagenesis) with respect to the total calcite (foraminifer + diagenetic), and estimate its concentration of %Mg based on the peak (104) angulare position. The values in roman font correspond to samples already analyzed in the study by *Boussetta et al.* [2011], while the values in italics indicate new samples from the present study.

[b]The relative amount (in %) of the Mg-rich calcite (Mg-rich calcite/(Mg-rich + Mg-poor calcite)) has been estimated based on the areas of the two calcite phases in the XRD profiles.

[c]Sites in which we conducted detailed Scanning Electron Microscope (SEM) investigations. Site V2, in the Tyrrhenian Sea, is located at the same location than site KET80–22; and sites B-109 and B-110 are located on the same site than core MD99–2344, in the Gulf of Lyon (see Figure 1).

[d]At several sites Mg-rich diagenetic calcite was not detected in XRD diagrams (n.d. = non detected).

using only *G. ruber* Mg/Ca data from the western Mediterranean Sea, we could find a significant relationship to calcification temperature, making it possible to validate Mg/Ca thermometry for paleoreconstruction in this part of the Mediterranean Sea at least. We plotted Mg/Ca values with respect to isotopic temperatures for the seventeen, western Mediterranean core tops including the two Atlantic samples. Interestingly, even with these selected core tops for which Mg/Ca values are in the expected correct range of Mg/Ca-thermometry, there is still no clear correlation between *G. ruber* Mg/Ca ratios and isotopic calcification temperatures (R^2 = 0.21 for an exponential fit; Figure 6a). Furthermore, the global Mg/Ca trend with increasing SST seems to be rather opposite to what is expected, showing no coherence with the *G. ruber* Mg/Ca-T calibration from the open ocean [*Anand et al.*, 2003].

4. Discussion

4.1. Potential Sources of Mg/Ca Bias in Our Western Mediterranean Sites: Dissolution at Depth and Possible Bias by Surface Water pH or [$CO_3^{=}$]

[32] Dissolution at the seafloor is well known to affect the Mg/Ca of deposited foraminifer shells [*Brown and Elderfield*, 1996; *Dekens et al.*, 2002; *Rosenthal et al.*, 2003; *Nouet and Bassinot*, 2007; *Hoogakker et al.*, 2009]. However, at our western Mediterranean sites, bottom water [$CO_3^{=}$] is high, and calculation of saturation states relative to calcite clearly shows that bottom water is always supersaturated relative to calcite. The lack of dissolution is also confirmed through visual inspection of samples, which shows no evidence of foraminifer shell modifications or assemblage changes that could be related to dissolution processes.

[33] Mg/Ca data from core top material retrieved in the Atlantic Ocean suggest that the incorporation of Mg in the calcite shell of *G. ruber* could respond to surface water pH or carbonate ion content of surface water [*Arbuszewski et al.*, 2008]. However, recent culture experiments [*Kisakürek et al.*, 2008] and other core top studies concluded that the influence of pH or surface [$CO_3^{=}$] on planktonic foraminifer Mg/Ca ratios is negligible at ambient seawater pH [*Cléroux*, 2007; *Cléroux et al.*, 2008; *Mathien-Blard and Bassinot*, 2009]. We tested the possible effect of pH and [$CO_3^{=}$] of our *G. ruber* Mg/Ca data set using *Archer* [1996] gridded Atlas, but found no significant effect.

4.2. Can We Confidently Use Calcification Isotopic Temperature for the Empirical Calibration of *Globigerinoides ruber* Mg/Ca in the Mediterranean Sea?

[34] To look for the Mg/Ca –temperature relationship of *G. ruber*, we used the isotopic calcification temperatures obtained from *G. ruber* $\delta^{18}O_f$ and the salinity-derived $\delta^{18}O_w$ of seawater. This approach has been adopted in several other studies dealing with empirical Mg/Ca-T calibration [i.e., *Elderfield and Ganssen*, 2000; *Elderfield et al.*, 2002; *Anand et al.*, 2003; *Cléroux et al.*, 2009; *Mathien-Blard and Bassinot*, 2009, *Regenberg et al.*, 2009]. Yet, according to *Ferguson et al.* [2008], the isotopic temperature approach is complicated by the pres-

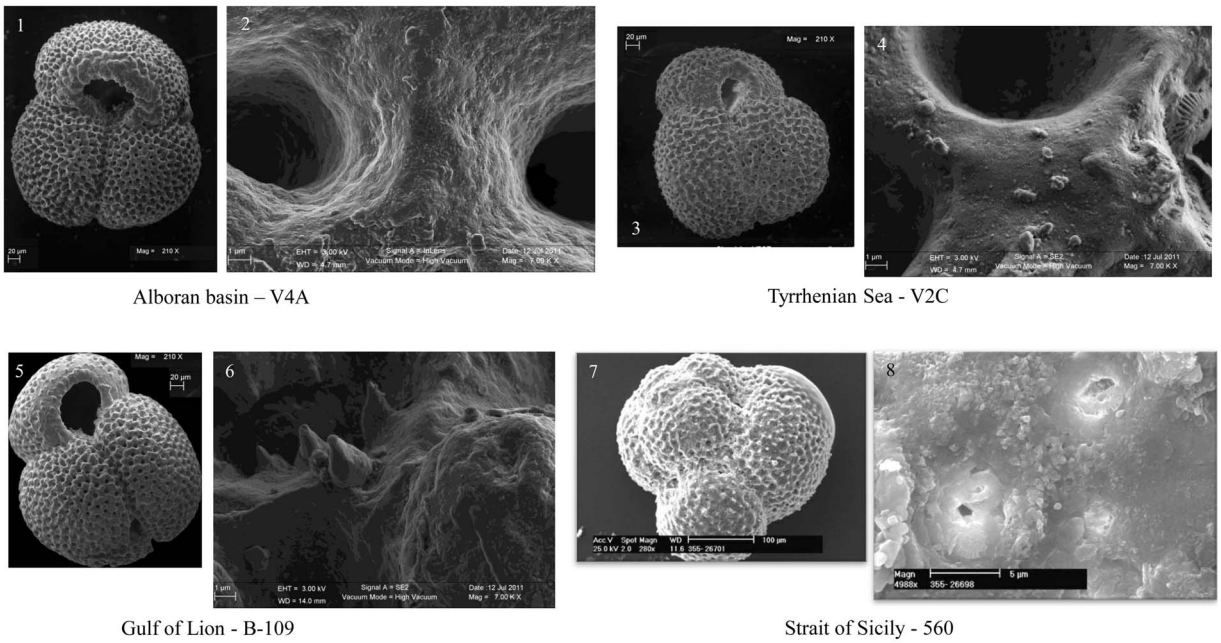

Figure 5. SEM images of the exterior of specimens of *Globigerinoides ruber* (white) picked in surface sediments (0–0.5 cm) retrieved from the Mediterranean seafloor. 1) one specimen from Site V4A (Alboran Sea; ×210); 2) detail of image 1 (×7000) showing the well-preserved, glassy texture of the test; 3) one specimen from site V2C (Tyrrhenian Sea; ×210); 4) detail of specimen from image 3 (×7000) showing the well-preserved, glassy texture of the test; 5) one specimen from site B109 (Gulf of Lyon; ×210); 6) detail of image 5 (×7000) showing light evidence of re-crystallization (rhombohedral calcite overgrowth); 7) a specimen from Site 560 (Eastern Mediterranean Sea; from *Boussetta et al.* [2011]; ×280); 8) detailed of image 7, showing evidence of intense re-crystallization (pores are closed, coccoliths glued to the surface of the test; numerous well-crystallized (rhombohedral), calcite overgrowths). Sample V4A is a box corer replicate collected from the site V4, see Figure 1; sample V2C come from the same oceanographic campaign and is a box corer replicate collected from the site V2 in the Tyrrhenian Sea during the TRANSMED (TMC-07) cruise and its geographical position is comparable to site sample KET80–22, see Figure 1; the same situation for the sample B-109 which geographical position is comparable to site sample MD99–2344 in the Gulf of Lyon.

ence of vital effects, which vary from species to species and with region, and which result in offsets from pure thermodynamic behavior during oxygen isotope incorporation. In the Mediterranean Sea, estimates for the vital offsets in foraminifera species are not generally available, with the exception of some modeled results [*Rohling et al.*, 2004]. In addition, *Ferguson et al.* [2008] suggest that applying the isotopic thermometer on Mediterranean foraminifers is made even more difficult due to large seasonal changes in sea surface $\delta^{18}O_w$ (to 1 (psu) [*MEDAR Group*, 2002]) and the paucity of $\delta^{18}O_w$ database available to constrain this variability. Thus, *Ferguson et al.* [2008] preferred to use World Ocean Atlas 2005 data [*Locarnini et al.*, 2006], averaged over the observed depth habitats and peak seasonal abundances for the Mediterranean [*Pujol and Vergnaud-Grazzini*, 1995]. Using this approach with our own western Mediterranean sites and comparing *G. ruber* Mg/Ca data relative to Atlas derived temperatures, instead of isotopic temperatures, does not improve the Mg/Ca-SST correlation. Using the Atlas derived temperatures, the correlation coefficient (R^2) drops to 0.07 (Figure 6b), whereas it reaches 0.21 when using isotopic temperatures (Figure 6a). Our data suggest, therefore, that the lack of consistent relationship between Mg/Ca and SST is not an artifact associated to our choice of using isotopic temperatures instead of Atlas-derived temperatures.

4.3. Salinity Effect on *Globigerinoides ruber* Mg/Ca

[35] Recent studies have emphasized the potential role of salinity as a bias on Mg/Ca thermometry [*Ferguson et al.*, 2008; *Kisakürek et al.*, 2008; *Mathien-Blard and Bassinot*, 2009; *Arbuszewski et al.*, 2010]. In order to evaluate the possibility that *G. ruber* Mg/Ca data from western Mediterranean Sea core tops are affected by salinity, we followed the approach developed by *Mathien-Blard and Bassinot* [2009]. These authors relied

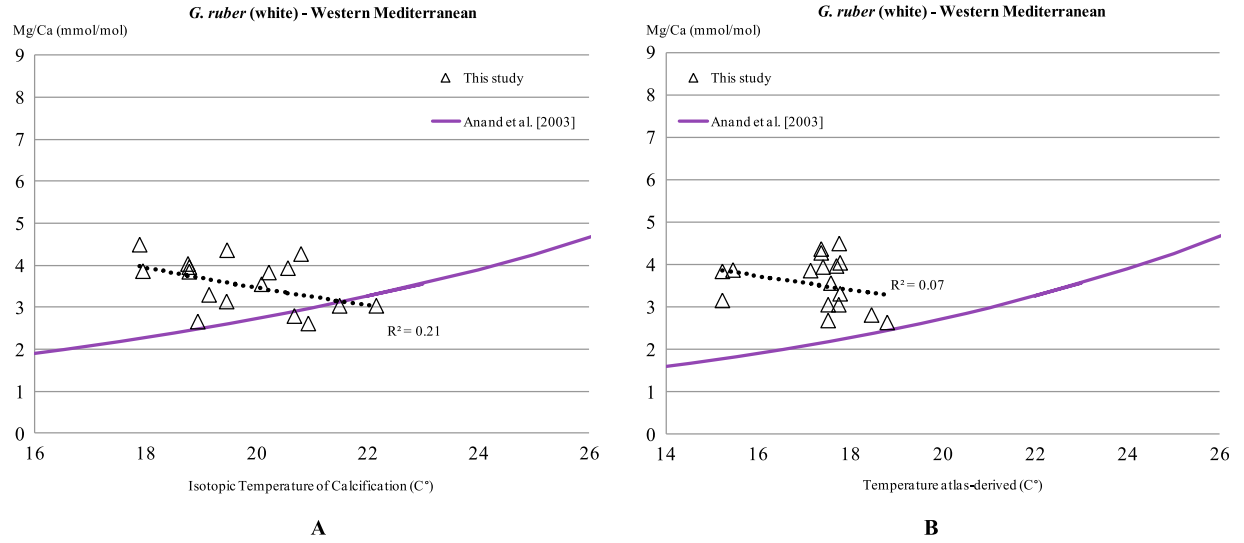

Figure 6. (a) *G. ruber* (white) Mg/Ca ratios plotted against $\delta^{18}O_w$-derived isotopic temperatures calculated using the equations of *Shackleton* [1974]. (b) *G. ruber* (white) Mg/Ca ratios plotted against atlas-derived isotopic temperatures. The exponential regression, derived from taking into account all core top data from the Western Mediterranean samples, is shown in dark. Purple curve is existing calcification temperature calibration for *G. ruber* from the sediment trap series located in the Sargasso Sea; *Anand et al.* [2003] $Mg/Ca = 0.449\ ^{e\ 0.09T}$.

on the empirical calibration of *G. ruber* Mg/Ca to isotopic calcification temperatures (T_{iso}) performed in the Atlantic Ocean by *Anand et al.* [2003]. Then, they simply proposed to look at the salinity effect by analyzing the potential shift between the estimated $T_{Mg/Ca}$ and the reference T_{iso}.

[36] Following this approach, we calculated, at all of our sites, the difference (ΔT) between Mg/Ca-temperature ($T_{Mg/Ca}$) and the isotopic temperature (T_{iso}), and compared ΔT to SSS. For this purpose, the Mg/Ca of *G. ruber* was converted to sea surface temperature based on *Anand et al.*'s [2003] empirical equation developed for *G. ruber* picked in the size fraction 250–315 μm.

$$T_{Mg/Ca} = \ln(Mg/Ca/0.449)/0.09 \quad \text{for } G.\,ruber \qquad (4)$$

We chose to use *Anand et al.*'s [2003] Mg/Ca thermometry calibration for two reasons. First, their empirical relationship to temperature was obtained using the same isotopic temperature equation than the one we used here [*Shackleton*, 1974]. In addition, *Anand et al.* [2003] have used the same cleaning protocol as we did in this work [*Barker et al.*, 2003]. This aspect is important since an inter-laboratory calibration exercise have clearly showed that the cleaning protocol has a noticeable effect on Mg/Ca results [*Rosenthal et al.*, 2004].

[37] In our database ΔT (= $T_{Mg/Ca}$-T_{iso}) varies from −2°C in the Atlantic Ocean to +8°C in the Western Mediterranean Sea. When plotted versus SSS, our ΔT values show a clear, positive trend with a rather good correlation coefficients despite some level of scattering ($R^2 = 0.61$; *** = $P \ll 0.001$; Figure 7a). We decided to plot our data together with those obtained from Indo-Pacific and Atlantic core tops by *Mathien-Blard and Bassinot* [2009], and which cover a much larger salinity range. Interestingly, despite the higher level of scattering, our western Mediterranean ΔT appear to be coherent with Indo-Pacific and Atlantic core top data (Figure 7b). The linear regression calculated through the combined data set, shows a good correlation coefficient ($R^2 = 0.71$) and correspond to the following equation:

$$\Delta T = 1.72 * SSS - 61.15 \qquad (5)$$

The slope of the equation (5) indicates that a salinity change of +1 (psu) change in salinity would induce a ~+1.7°C change in $T_{Mg/Ca}$(bias) relative to the isotopic calcification temperature (this equates to about ~15% Mg/Ca change per unit salinity change increase). ΔT equals 0 ($T_{iso} = T_{Mg/Ca}$) for a salinity of ~35.6 (psu). Below this threshold of salinity, $T_{Mg/Ca}$ are lower than T_{iso} and they are higher than T_{iso} for salinity above ~35.5 (psu) (Figure 7). Thus, despite a higher level of scattering, it clearly seems that western Mediterranean Sea *G. ruber* Mg/Ca data confirm the salinity bias on Mg/Ca-thermometry evidenced using Atlantic and Indo-Pacific core tops [*Mathien-Blard and Bassinot*, 2009].

[38] Concerning the vertical dispersion of western Mediterranean data (see Figure 7b), it is likely that – at least partially - this could result from the limited and heterogeneous imprint of Mg-rich diagenesis on samples from this area. Our conclusions that diagenesis does not seem to cancel out totally the original, sea surface Mg/Ca signal and that it mainly affects the "second-order" variability (scattering), will need to be tested in future studies by using more powerful methods such as, for instance, the Flow-Through Time Resolved (FT-TRA) approach developed at OSU [*Klinkhammer et al.*, 2004].

4.4. Salinity Effect on Mg/Ca: Discrepancy Between Core Top and Laboratory Culture Results

[39] The existence of a salinity effect on planktonic foraminifer Mg/Ca is also in general agreement with culture experiments or other core top studies [i.e., *Nürnberg et al.*, 1996; *Lea et al.*, 1999; *Ferguson et al.*, 2008; *Groeneveld et al.*, 2008; *Kisakürek et al.*, 2008; *Dueñas-Bohórquez et al.*, 2009; *Kontakiotis et al.*, 2009; *Sadekov et al.*, 2009; *Arbuszewski et al.*, 2010]. Yet, the sensitivity of Mg/Ca to salinity changes differs markedly from one study to another. Our results are coherent with core top studies of *Mathien-Blard and Bassinot* [2009] and *Arbuszewski et al.* [2010], which both suggest a ~15% change per unit change in salinity. This is only slightly higher than the 11% change per unit change in salinity established for another planktonic species, *G. sacculifer*, based on culture experiments [*Nürnberg et al.*, 1996; *Dueñas-Bohórquez et al.*, 2009], but it is significantly higher than the 5% sensitivity estimated for *G. ruber* from culture [*Kisakürek et al.*, 2008]. Based on its $\delta^{18}O$ record, *Groeneveld et al.* [2008] interpreted the high Mg/Ca ratios (>7 mmol/mol) measured in an ODP site from the Caribbean Sea as related to SSS.

[40] The reason for the discrepancy between culture results and core top calibrations has not been clearly addressed yet. *Kisakürek et al.* [2008] - referring to *Ferguson et al.*'s [2008] data - explain the much steeper slope obtained from Mediterranean foraminifers compared to culture results, as due to the precipitation of inorganic calcite within bottom sediments or in the water column causing shell Mg/Ca ratios to increase. As we have seen above, this explanation may be valid when considering Mg/Ca-SST calibrations performed over the entire Mediterranean Sea, for which a clear diagenetic contamination exists in the central and eastern basins. However, when considering data from the western Mediterranean sites only, this explanation is unlikely. We have shown that Mg/Ca data obtained in this area and the salinity effect that can be deduced, are in agreement with results from Indo-Pacific and Atlantic sites, for which no overgrowth of Mg-rich calcite has been described [*Arbuszewski et al.*, 2008; *Mathien-Blard and Bassinot*, 2009]. *Barker et al.* [2005] suggested that culture experiments may not sufficiently reproduce the natural environment conditions, which may induce a potential stress on foraminifers, possibly affecting the calcification of the chambers. Uncertainty in culture calibrations may arise, therefore, if differences in Mg/Ca during shell growth are caused by changing biological controls rather than solely by changes in temperature or salinity. In any case, even if the discrepancy between culture and core top results is not fully understand, Mg/Ca-SST calibrations and salinity bias derived from core top material are extremely valuable for paleoceanographic reconstructions since they are based on the same material that will eventually form the sedimentary record.

4.5. Paleoceanographic Implications: Addressing the Reliability of the Mg/Ca Thermometer for Mediterranean Reconstructions

[41] As we have seen above, in the Mediterranean Sea, post-depositional alteration results in the development of an early diagenetic, Mg-rich (~10–12% $MgCO_3$) calcite coating, which can constitute up to 20% of the total shell calcite in the central and eastern Mediterranean basin. The protocol of *Barker et al.* [2003] used for the sample preparation for the Mg/Ca analysis, is clearly insufficient in removing and cleaning with accuracy this diagenetic deposit that continues to pollute the Mg/Ca ratios measured from ICP-AES analyses. The resulting Mg/Ca values measured from our ICP-AES method range from 2.6 mmol/mol to clearly anomalous values as high as 35.5 mmol/mol (Table 2), with a high degree of scattering.

[42] Alternative cleaning method that contains a reductive step can help removing this high-Mg coating [*Yu et al.*, 2007; *Hoogakker et al.*, 2009] clearly showed that the citrate used for this reductive cleaning step results in the preferential leaching of Mg-rich parts of benthic foraminiferal shells. Yet, there is no real control on the exact amount of Mg-rich calcite dissolved. Thus, a more powerful alternative for well constrained and accurate Mg/Ca thermometry in the Mediterranean Sea might be the

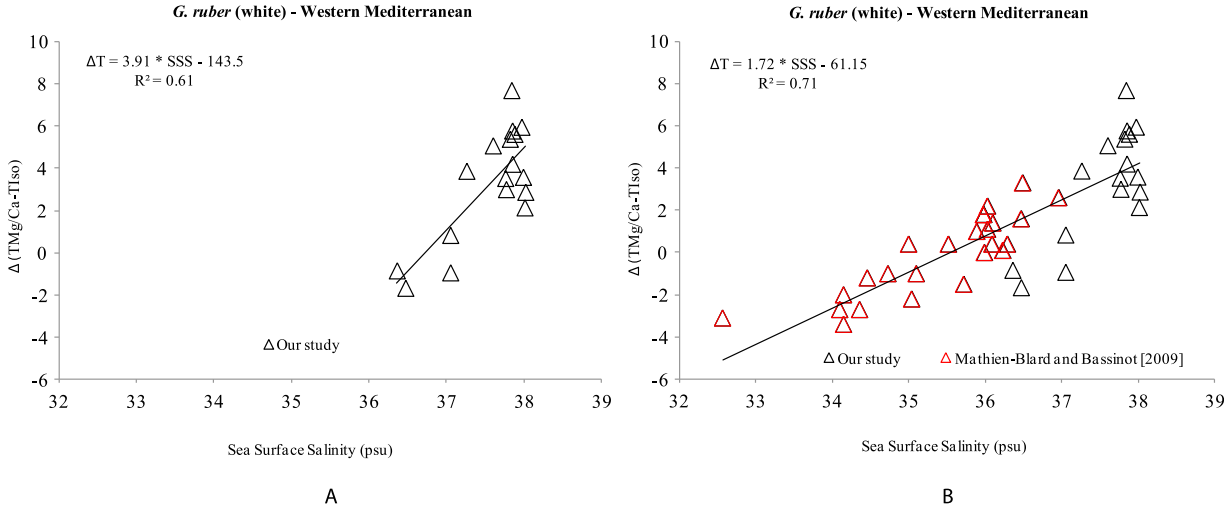

Figure 7. (a) Series of our Western Mediterranean ΔT (= $T_{Mg/Ca} - T_{iso}$) plotted against atlas-derived sea surface salinities [*MEDAR Group*, 2002] and [*Antonov et al.*, 2006] for *G. ruber* (white). (b) Series of ΔT (= $T_{Mg/Ca} - T_{iso}$) plotted against atlas-derived sea surface salinities [*MEDAR Group*, 2002] and [*Antonov et al.*, 2006] for *G. ruber* (white). Temperatures corresponding Mg/Ca ratios were calculated based on calibration from *Anand et al.* [2003] as explained in the text. ΔT is the difference between $T_{Mg/Ca}$ and T_{iso} calculated from $\delta^{18}O_w$-derived isotopic temperatures calculated using the equation of *Shackleton* [1974]. West Mediterranean core tops are symbolized by black triangles; Indo-Pacific and North Atlantic core tops analyzed by *Mathien-Blard and Bassinot* [2009] are shown as red triangles. The black line materializes the linear regression calculated taking into account all the data on the graphic and for both Figures 7a and 7b, it results highly significant (*** = $P \ll 0.001$).

use of Flow-Through Time Resolved (FT-TRA) method developed at the Oregon State University [*Klinkhammer et al.*, 2004]. This approach dissolves progressively the foraminiferal shell and make possible to separate Mg contributions from various calcitic phases, since Mg-rich phases will dissolve more rapidly than Mg-poor phases. This technique has been recently tested by *Boussetta et al.* [2011] using four core tops from the Mediterranean basin. These authors obtained Mg/Ca values significantly lower than those obtained by conventional ICP-AES analysis with an improved homogeneity. Further studies are required to confirm the potential of the FT-TRA technique.

[43] In the western Mediterranean basin (including the two Atlantic samples), the Mg/Ca values vary from ~2 to ~5 mmol/mol, showing a typical open-ocean range. XRD do not reveal the presence of Mg-rich calcite, but.SEM observations suggested the occurrence of little amount of recrystallization in a few areas, associated to inter-sample heterogeneity. Such diagenetic imprint is likely associated to Mg/Ca scattering, but it does not cancel out totally the initial Mg/Ca signal, which reveals a significant relationship to sea surface salinity, which bias the expected temperature effect. This salinity effect is coherent with recent results obtained on Indo-Pacific and Atlantic surface sediments, which suggest that a +1 change in salinity (psu) results in a +1.7°C Mg/Ca-temperature bias [*Mathien-Blard and Bassinot*, 2009; *Arbuszewski et al.*, 2010]. *Mathien-Blard and Bassinot* [2009] developed a correction procedure applied to $T_{Mg/Ca}$ and $\delta^{18}O_f$ measured on *G. ruber* in order to derive sea surface temperatures and $\delta^{18}O_{sw}$ corrected for the salinity effect on Mg/Ca. This method rests upon regional (evaporation/precipitation) and global (ice sheet) SSS-$\delta^{18}O_{sw}$ relationships established for the modern ocean. In order to apply this correction for paleoceanographic reconstructions, the necessary assumption is that the regional SSS-$\delta^{18}O_{sw}$ relationship remains invariant through time. In the Indian Ocean, this assumption was validated by model results [*Delaygue et al.*, 2001]. Yet, such an assumption could be wrong for the Mediterranean Sea, which is a semi-enclosed basin for which SSS-$\delta^{18}O_{sw}$ depends not only on the hydrological cycle but also on the exchanges of water with the Atlantic Ocean. The modern regional SSS- $\delta^{18}O_{sw}$ equation for the Mediterranean area obtained by *Kallel et al.* [1997] has been used successfully for paleoceanographic reconstructions over the Holocene, suggesting that – at least over this period of time – the correction procedure developed by *Mathien-Blard and Bassinot* [2009] should be valid.

[44] Additional work is mandatory to check whether salinity of the ambient water also affects significantly the Mg/Ca of other planktonic species in the region (i.e., *G. bulloides* and *O. universa*) and its implications in the hydrographic reconstructions. Differences with *van Raden et al.* [2011]'s observations suggest that diagenesis may have a different impact on foraminifer species in relation to test morphology or microstructure.

5. Conclusions

[45] Our data shows that Mg/Ca ratio in *G. ruber* shells retrieved from box corer and core tops of the semi-enclosed, Mediterranean Sea reach much higher values and show a stronger scattering than those obtained in open oceans. The level of scattering and high values we obtained are similar to what can be observed in the data set from *Ferguson et al.* [2008].

[46] SEM observations and XRD analyses show the presence of a Mg-rich calcite (10–12% $MgCO_3$) coating, particularly in the central and eastern Mediterranean Sea where this calcite coating can represent up to ~20% of the total *G. ruber* calcite. Such a Mg-rich calcite is typical of early diagenetic calcite deposition, in equilibrium with seawater Mg and Ca composition.

[47] In the western Mediterranean Sea, Mg-rich calcite is not detected by the XRD analyses. If it present, it is therefore in small amounts (<0.5%).

[48] SEM observations performed on *G. ruber* shells picked from western Mediterranean sea samples reveal the absence of diagenetic imprint in several areas (i.e., Alboran Sea), and the occurrence of limited recrystallization in samples from the Gulf of Lyon and the Tyrrhennian Sea, with important inter-sample heterogeneity. Due to the limited extension of recrystallization, it is likely that most of the Mg-rich calcite can be removed during the Mg/Ca cleaning protocol. Yet, some part of the Mg/Ca scattering in the western Mediterranean Sea may be attributed to remains of Mg-rich calcite (as only minute amounts of this calcite that contains 10–12 mol% Mg car significantly alter Mg/Ca data).

[49] Using only those western Mediterranean sea samples, there is no immediate and clear correlation between Mg/Ca and isotopic calcification temperatures (estimated from *G. ruber* $^{18}O_f$ and using modern seawater $\delta^{18}O_{sw}$). Comparing our data with those obtained on the open ocean (Atlantic and Indo-Pacific [*Mathien-Blard and Bassinot*, 2009]), suggests that salinity creates a major bias on Mg/Ca-thermometry, with a +1 change in salinity (psu) resulting in an ~+1.7°C shift in temperature estimated from Mg/Ca ratio in the Western Mediterranean basin. This is, however, a much steeper relation to salinity than what has been evidenced from *G. ruber* culture experiments [*Kisakürek et al.*, 2008].

[50] One should be extremely cautious when using Mg/Ca in the Mediterranean Sea for paleotemperature reconstructions. Our results suggest that accurate paleo-reconstructions in the central and eastern Mediterranean Sea are probably impossible with conventional methods due to the strong overprint associated to the diagenetic deposition of a Mg-rich calcite. As shown by *Boussetta et al.* [2011], using the FT-TRA approach [*Klinkhammer et al.*, 2004] to measure Mg/Ca is likely the only way to get reliable Mg/Ca data in this area.

Acknowledgments

[51] We thank the Laboratoire des Sciences du Climat et de l'Environnement (LSCE-CNRS/CEA/UVSQ) for providing laboratory facilities and Annachiara Bartolini from the Muséum Nationale d'Histoire Naturelle for the photos at SEM. The authors gratefully acknowledge Francesco Falcieri (Polytechnic University of Marche), who provided and elaborated hydrological and oceanographic data of the Mediterranean Sea and graphical map solution. Giuseppe Siani and Michel Fontugne are thanked for constructive discussions and Elisabeth Michel for critical assessment of the manuscript. We thank François Guichard who provided additional sediment samples. Support for this research is provided by the "Luigi e Francesca Brusarosco" Award for the foreign country stays of Italian researchers in the field of environmental sciences. This work was also supported by the ANR-LAMA project.

References

Allison, N., and W. E. N. Austin (2003), The potential of ion microprobe analysis in detecting geochemical variations across individual foraminifera tests, *Geochem. Geophys. Geosyst.*, *4*(2), 8403, doi:10.1029/2002GC000430.

Anand, P., H. Elderfield, and M. H. Conte (2003), Calibration of Mg/Ca thermometry in planktonic foraminifera from a sediment trap time series, *Paleoceanography*, *18*(2), 1050, doi:10.1029/2002PA000846.

Antonov, J., R. Locarnini, T. P. Boyer, A. V. Mishonov, and H. E. Garcia (2006), *World Ocean Atlas, 2005*, vol. 2, *Salinity*, *NOAA Atlas NESDIS*, vol. 62, edited by S. Levitus, 182 pp., NOAA, Silver Spring, Md.

Arbuszewski, J., P. Demenocal, and A. Kaplan (2008), Towards a global calibration and validation of the *G. ruber* (white) Mg/Ca paleothermometer, *Eos Trans. AGU*, *89*(53), Fall Meet. Suppl., Abstract PP41F-02.

Arbuszewski, J., P. Demenocal, A. Kaplan, and E. C. Farmer (2010), On the fidelity of shell-derived $\delta^{18}O$ seawater estimates, *Earth Planet. Sci. Lett.*, *300*, 185–196, doi:10.1016/j.epsl.2010.10.035.

Archer, D. (1996), An atlas of the distribution of calcium carbonate in sediments of the deep sea, *Global Biogeochem. Cycles*, *10*, 159, doi:10.1029/95GB03016.

Barker, S., M. Greaves, and H. Elderfield (2003), A study of cleaning procedures used for foraminiferal Mg/Ca paleothermometry, *Geochem. Geophys. Geosyst.*, *4*(9), 8407, doi:10.1029/2003GC000559.

Barker, S., I. Cacho, H. Benway, and K. Tachikawa (2005), Planktonic foraminiferal Mg/Ca as a proxy for past oceanic temperatures: A methodological overview and data compilation for the Last Glacial Maximum, *Quat. Sci. Rev.*, *24*, 821–834, doi:10.1016/j.quascirev.2004.07.016.

Boussetta, S., F. Bassinot, A. Sabbatini, N. Caillon, J. Nouet, N. Kallel, H. Rebaubier, G. Klinkhammer, and L. Labeyrie (2011), Diagenetic Mg-rich calcite in Mediterranean sediments: Quantification and impact on foraminiferal Mg/Ca thermometry, *Mar. Geol.*, *280*(1–4), 195–204, doi:10.1016/j.margeo.2010.12.011.

Brown, S., and H. Elderfield (1996), Variations in Mg/Ca and Sr/Ca ratios of planktonic foraminifera caused by postdepositional dissolution: Evidence of shallow Mg-dependent dissolution, *Paleoceanography*, *11*, 543–552, doi:10.1029/96PA01491.

Cléroux, C. (2007), Variabilité au cours des derniers 20000 ans de l'hydrologie de l'Atlantique tropical Nord et de l'actvité du Gulf Stream à partir de la composition isotopique de l'oxygène et de la composition en éléments trace des foraminifères planctoniques profonds, Ph.D. thesis, 163 pp., Univ. Paris XI, Orsay, Paris.

Cléroux, C., E. Cortijo, P. Anand, L. Labeyrie, F. Bassinot, N. Caillon, and J.-C. Duplessy (2008), Mg/Ca and Sr/Ca ratios in planktonic foraminifera: Proxies for upper water column temperature reconstruction, *Paleoceanography*, *23*, PA3214, doi:10.1029/2007PA001505.

Cléroux, C., J. Lynch-Stieglitz, M. W. Schmidt, E. Cortijo, and J.-C. Duplessy (2009), Evidence for calcification depth change of *Globorotalia truncatulinoides* between deglaciation and Holocene in the Western Atlantic Ocean, *Mar. Micropaleontology*, *73*(1–2), 57–61, doi:10.1016/j.marmicro.2009.07.001.

Dekens, P. S., D. W. Lea, D. K. Pak, and H. J. Spero (2002), Core top calibration of Mg/Ca in tropical foraminifera: Refining paleotemperature estimation, *Geochem. Geophys. Geosyst.*, *3*(4), 1022, doi:10.1029/2001GC000200.

Delaygue, G., E. Bard, and C. Rollion (2001), Oxygen isotope/salinity relationship in the northern Indian Ocean, *J. Geophys. Res.*, *106*(C3), 4565–4574, doi:10.1029/1999JC000061.

de Villiers, S., M. Greaves, and H. Elderfield (2002), An intensity ratio calibration method for the accurate determination of Mg/Ca and Sr/Ca of marine carbonates by ICP-AES, *Geochem. Geophys. Geosyst.*, *3*(1), 1001, doi:10.1029/2001GC000169.

Dueñas-Bohórquez, A., R. Elisabeth da Rocha, A. Kuroyanagi, J. Bijma, and G.-J. Reichart (2009), Effect of salinity and seawater calcite saturation state on Mg and Sr incorporation in cultured planktonic foraminifera, *Mar. Micropaleontology*, *73*, 178–189, doi:10.1016/j.marmicro.2009.09.002.

Duplessy, J. C., L. Labeyrie, A. Juillet-Leclerc, F. Maitre, J. Duprat, and M. Sarnthein (1991), Surface salinity reconstruction of the North Atlantic Ocean during the Last Glacial Maximum, *Oceanol. Acta*, *14*, 311–324.

Eggins, S., P. De Deccker, and J. Marshall (2003), Mg/Ca variation in planktonic foraminifera tests: Implications for reconstructing palaeo-seawater temperature and habitat migration, *Earth Planet. Sci. Lett.*, *212*, 291–306, doi:10.1016/S0012-821X(03)00283-8.

Elderfield, H., and G. Ganssen (2000), Past temperature and $\delta^{18}O$ of surface ocean waters inferred from foraminiferal Mg/Ca ratios, *Nature*, *405*, 441–445.

Elderfield, H., M. Vautravers, and M. Cooper (2002), The relationship between shell size and Mg/Ca, Sr/Ca, $\delta^{18}O$, and $\delta^{13}C$ of species of planktonic foraminifera, *Geochem. Geophys. Geosyst.*, *3*(8), 1052, doi:10.1029/2001GC000194.

Ferguson, J., G. Henderson, M. Kucera, and R. Rickaby (2008), Systematic change of foraminiferal Mg/Ca ratios across a strong salinity gradient, *Earth Planet. Sci. Lett.*, *265*, 153–166, doi:10.1016/j.epsl.2007.10.011.

Gehlen, M., F. Bassinot, L. Beck, and H. Khodja (2004), Trace element cartography of *Globigerinoides ruber* shells using particle-induced X-ray emission, *Geochem. Geophys. Geosyst.*, *5*, Q12D12, doi:10.1029/2004GC000822.

Greaves, M., et al. (2008), Interlaboratory comparison study of calibration standards for foraminiferal Mg/Ca thermometry, *Geochem. Geophys. Geosyst.*, *9*, Q08010, doi:10.1029/2008GC001974.

Groeneveld, J., D. Nürnberg, R. Tiedemann, G. Reichart, S. Steph, L. Reuning, D. Crudeli, and P. Mason (2008), Foraminiferal Mg/Ca increase in the Caribbean during the Pliocene: Western Atlantic Warm Pool formation, salinity influence, or diagenetic overprint?, *Geochem. Geophys. Geosyst.*, *9*, Q01P23, doi:10.1029/2006GC001564.

Hoogakker, B. A. A., G. P. Klinkhammer, H. Elderfield, E. J. Rohling, and C. Hayward (2009), Mg/Ca paleothermometry in high salinity environments, *Earth Planet. Sci. Lett.*, *284*, 583–589, doi:10.1016/j.epsl.2009.05.027.

Kallel, N., M. Paterne, J. C. Duplessy, C. Vergnaud-Grazzini, C. Pujol, L. Labeyrie, M. Arnold, M. Fontugne, and C. Pierre (1997), Enhanced rainfall in the Mediterranean region during the last sapropel event, *Oceanol. Acta*, *20*(5), 697–712.

Kisakürek, B., A. Eisenhauer, F. Böhm, D. Garbe-Schönberg, and J. Erez (2008), Controls on shell Mg/Ca and Sr/Ca in cultured planktonic foraminiferan, *Globigerinoides ruber* (white), *Earth Planet. Sci. Lett.*, *273*, 260–269, doi:10.1016/j.epsl.2008.06.026.

Klinkhammer, G. P., B. A. Haley, A. C. Mix, H. M. Benway, and M. Cheseby (2004), Evaluation of automated flow-through time-resolved analysis of foraminifera for Mg/Ca paleothermometry, *Paleoceanography*, *19*, PA4030, doi:10.1029/2004PA001050.

Kontakiotis, G., A. Antonarakou, P. G. Mortinm, M. V. Triantaphyllou, M. Á. Martínez-Botí, and M. D. Dermitzakis (2009), Assessing the salinity effect on planktonic foraminiferal Mg/Ca: Evidence from Aegean Sea core-top samples (Eastern Mediterranean), *Geophys. Res. Abstr.*, *11*, EGU2009–EGU1301.

Kucera, M., et al. (2005), Reconstruction of sea-surface temperatures from assemblages of planktonic foraminifera: Multi-technique approach based on geographically constrained calibration data sets and its application to glacial Atlantic and Pacific oceans, *Quat. Sci. Rev.*, *24*(7–9), 951–998, doi:10.1016/j.quascirev.2004.07.014.

Lea, D., T. Mashiotta, and H. Spero (1999), Controls on magnesium and strontium uptake in planktonic foraminifera determined by live culturing, *Geochim. Cosmochim. Acta*, *63*, 2369–2379, doi:10.1016/S0016-7037(99)00197-0.

Levi, C., L. Labeyrie, F. Bassinot, F. Guichard, E. Cortijo, C. Waelbroeck, N. Caillon, J. Duprat, T. de Garidel-Thoron, and H. Elderfield (2007), Low-latitude hydrological cycle and rapid climate changes during the last deglaciation, *Geochem. Geophys. Geosyst.*, *8*, Q05N12, doi:10.1029/2006GC001514.

Locarnini, R. A., A. V. Mishonov, J. I. Antonov, T. P. Boyer, and H. E. Garcia (2006), *World Ocean Atlas 2005*, vol. 1, *Temperature*, *NOAA Atlas NESDIS*, vol. 61, edited by S. Levitus, 182 pp., NOAA, Silver Spring, Md.

Mashiotta, T., D. Lea, and H. Spero (1999), Glacial-interglacial changes in Subantarctic sea surface temperature and δ^{18}O-water using foraminiferal Mg, *Earth Planet. Sci. Lett.*, *170*, 417–432, doi:10.1016/S0012-821X(99)00116-8.

Mathien-Blard, E., and F. Bassinot (2009), Salinity bias on the foraminifera Mg/Ca thermometry: Correction procedure and implications for past ocean hydrographic reconstructions, *Geochem. Geophys. Geosyst.*, *10*, Q12011, doi:10.1029/2008GC002353.

MEDAR Group (2002), MEDATLAS/2002 database: Mediterranean and Black Sea database of temperature, salinity and bio-chemical parameters in climatological atlas [CD-ROM], Fr. Res. Inst. for Exploit. of Sea, Issy-les-Moulineaux, France. [Available at http://www.ifremer.fr/medar/.]

Morse, J. W., and F. T. Mackenzie (1990), Geochemistry of sedimentary carbonates, *Dev. Sedimentol.*, *48*, 1–707, doi:10.1016/S0070-4571(08)70330-3.

Morse, J. W., D. K. Gledhill, and F. J. Millero (2003), $CaCO_3$ precipitation kinetics in waters from the Great Bahamas Bank: Implications for the relationship between Bank hydrochemistry and whiting, *Geochim. Cosmochim. Acta*, *67*, 2819–2826, doi:10.1016/S0016-7037(03)00103-0.

Mucci, A. (1987), Influence of temperature on the composition of magnesian calcite overgrowths precipitated from seawater, *Geochim. Cosmochim. Acta*, *51*, 1977–1984, doi:10.1016/0016-7037(87)90186-4.

Nouet, J., and F. Bassinot (2007), Dissolution effects on the crystallography and Mg/Ca content of planktonic foraminifera *Globorotalia tumida* (Rotaliina) revealed by X-ray diffractometry, *Geochem. Geophys. Geosyst.*, *8*, Q10007, doi:10.1029/2007GC001647.

Nürnberg, D., J. Bijma, and C. Hemleben (1996), Assessing the reliability of magnesium in foraminiferal calcite as a proxy for water mass temperatures, *Geochim. Cosmochim. Acta*, *60*, 803–814, doi:10.1016/0016-7037(95)00446-7.

O'Neil, J. R., R. N. Clayton, and T. K. Mayeda (1969), Oxygen isotope fractionation in divalent metal carbonates, *J. Chem. Phys.*, *51*, 5547–5558, doi:10.1063/1.1671982.

Pujol, C., and C. Vergnaud-Grazzini (1995), Distribution patterns of live planktic foraminifera as related to regional hydrography and productive systems of the Mediterranean Sea, *Mar. Micropaleontology*, *25*(2–3), 187–217, doi:10.1016/0377-8398(95)00002-I.

Regenberg, M., D. Nürnberg, J. Schönfeld, and G. J. Reichart (2007), Early diagenetic overprint in Caribbean sediment cores and its effect on the geochemical composition of planktonic foraminifera, *Biogeosciences*, *4*, 957–973, doi:10.5194/bg-4-957-2007.

Regenberg, M., S. Steph, D. Nürnberg, R. Tiedemann, and D. Garbe-Schönberg (2009), Calibrating Mg/Ca ratios of multiple planktonic foraminiferal species with δ^{18}O-calcification temperatures: Paleothermometry for the upper water column, *Earth Planet. Sci. Lett.*, *278*, 324–336, doi:10.1016/j.epsl.2008.12.019.

Rohling, E., et al. (2004), Reconstructing past planktic foraminiferal habitats using stable isotope data: A case history for Mediterranean sapropel S5, *Mar. Micropaleontology*, *50*(1–2), 89–123, doi:10.1016/S0377-8398(03)00068-9.

Rosenthal, Y., D. W. Oppo, and B. K. Linsley (2003), The amplitude and phasing of climate change during the last deglaciation in the Sulu Sea, western equatorial Pacific, *Geophys. Res. Lett.*, *30*(8), 1428, doi:10.1029/2002GL016612.

Rosenthal, Y., et al. (2004), Interlaboratory comparison study of Mg/Ca and Sr/Ca measurements in planktonic foraminifera for paleoceanographic research, *Geochem. Geophys. Geosyst.*, *5*, Q04D09, doi:10.1029/2003GC000650.

Russell, A. D., B. Hönisch, H. J. Spero, and D. W. Lea (2004), Effects of seawater carbonate ion concentration and temperature on shell U, Mg, and Sr in cultured planktonic foraminifera, *Geochim. Cosmochim. Acta*, *68*(21), 4347–4361, doi:10.1016/j.gca.2004.03.013.

Sadekov, A., S. M. Eggins, P. de Deckker, U. Ninnemann, W. Kuhnt, and F. Bassinot (2009), Surface and subsurface seawater temperature reconstruction using Mg/Ca microanalysis of planktonic foraminifera *Globigerinoides ruber, Globigerinoides sacculifer*, and *Pulleniatina obliquiloculata*, *Paleoceanography*, *24*, PA3201, doi:10.1029/2008PA001664.

Schmidt, M., H. Spero, and D. Lea (2004), Links between salinity variation in the Caribbean and North Atlantic thermohaline circulation, *Nature*, *428*(6979), 160–163, doi:10.1038/nature02346.

Schmidt, M. W., M. J. Vautravers, and H. J. Spero (2006), Western Caribbean sea surface temperatures during the late Quaternary, *Geochem. Geophys. Geosyst.*, *7*, Q02P10, doi:10.1029/2005GC000957.

Sexton, P., P. Wilson, and P. Pearson (2006), Microstructural and geochemical perspectives on planktic foraminiferal preservation: "Glassy" versus "frosty," *Geochem. Geophys. Geosyst.*, *7*, Q12P19, doi:10.1029/2006GC001291.

Shackleton, N. J. (1974), Attainment of isotopic equilibrium between ocean water and benthonic foraminifera genus *Uvigerina*: Isotopic changes in the ocean during the last glacial, in *Les Méthodes Quantitatives d'étude des Variations du Climat au Cours du Pleistocène*, pp. 203–209, Cent. Natl. de la Rech. Sci., Gif-sur Yvette, France.

Thunell, R. C. (1978), Distribution of recent planktonic foraminifera in surface sediments of the Mediterranean Sea, *Mar. Micropaleontology*, *3*, 147–173, doi:10.1016/0377-8398(78)90003-8.

Tribble, J. S., and F. T. Mackenzie (1998), Recrystallization of magnesian calcite overgrowths on calcite seeds suspended in seawater, *Aquat. Geochem.*, *4*, 337–360, doi:10.1023/A:1009636331784.

Tribble, J. S., R. S. Arvidson, M. Lane III, and F. T. Mackenzie (1995), Crystal chemistry, and thermodynamic and kinetic properties of calcite, dolomite, apatite, and biogenic silica: Applications to petrologic problems, *Sediment. Geol.*, *95*, 11–37, doi:10.1016/0037-0738(94)00094-B.

van Raden, U. J., J. Groeneveld, M. Raitzsch, and M. Kucera (2011), Mg/Ca in the planktonic foraminifera *Globorotalia inflata* and *Globigerinoides bulloides* from Western Mediterranean plankton tow and core top samples, *Mar. Micropaleontology*, *78*, 101–112, doi:10.1016/j.marmicro.2010.11.002.

Waelbroeck, C., S. Mulitza, H. Spero, T. Dokken, T. Kiefer, and E. Cortijo (2005), A global compilation of late Holocene planktonic foraminiferal δ^{18}O: Relationship between surface water temperature and δ^{18}O, *Quat. Sci. Rev.*, *24*, 853–868, doi:10.1016/j.quascirev.2003.10.014.

Wollast, R., R. M. Garrels, and F. T. Mackenzie (1980), Calcite seawater reactions in ocean surface waters, *Am. J. Sci.*, *280*, 831–848, doi:10.2475/ajs.280.9.831.

Yu, J., H. Elderfield, M. Greaves, and J. Day (2007), Preferential dissolution of benthic foraminiferal calcite during laboratory reductive cleaning, *Geochem. Geophys. Geosyst.*, *8*, Q06016, doi:10.1029/2006GC001571.